Structural and Computational Studies of N-[(2,6-Diethylphenyl) carbamothioyl]-2,2-diphenylacetamide, N-[(3 Ethylphenyl) carbamothioyl]-2,2-diphenylacetamide and 2,2-Diphenyl-N-{[2-(trifluoromethyl) phenyl]carbamothioyl}acetamide

Ibrahim Abdul Razak, Suhana Arshad, Nur Rafikah Razali, Azhar Abdul Rahman, Mohd Sukeri Mohd Yusof

Abstract—Theoretical investigations are performed by DFT method of B3LYP/6-31G+(2d,p) and B3LYP/6-311G+(2d,p) basis sets for three carbonyl thiourea compounds, namely *N*-[(2,6-Diethylphenyl)carbamothioyl]-2,2-diphenylacetamide (Compound I), *N*-[(3-Ethylphenyl)carbamothioyl]-2,2-diphenylacetamide (Compound II) and 2,2-Diphenyl-*N*-{[2-(trifluoromethyl)phenyl]carbamothioyl}acetamide (Compound III). Theoretical calculations for bond parameters, harmonic vibration frequencies and isotropic chemical shifts are in good agreement with the experimental results. The calculated molecular vibrations show good correlation values, which are 0.998 and 0.999 with the experimental data. The energy gap for compounds I, II and III calculated at B3LYP/6-31G+(2d,p) basis set are 4.455866117, 4.297495791 and 4.313550514 eV respectively, while for B3LYP/6-311G+(2d,p) basis set the energy gap obtained are 4.453689205 (Compound I), 4.311373603 (Compound II) and 4.315727426 (Compound III) eV.

Keywords—Crystallization, DFT studies, Spectroscopic Analysis, Thiourea.

I. INTRODUCTION

THE molecular structure of carbonyl thiourea contains both hydrogen donors through the NH groups and acceptor centre through both carbonyl and thiocarbonyl groups that can coordinate with metal using oxygen and sulphur atoms [1], [2]. This capability of hydrogen bond formation has lead thiourea into numerous applications especially in medicinal and pharmacology field such as for antibreast cancer [3], [4], antifungal [5], [6], antimicrobial agents [7] and potential anti-influenza virus [8]. In recent years, the use of computational and theoretical studies by using Density Functional Theory (DFT) method has increased as this method helps to determine the molecular dipole moment, spectroscopic properties and molecular orbital analysis. The use of advanced calculation by applying the Beck's three parameters, Lee, Yang and Parr (B3LYP) approximation into the DFT method has improved the data accuracy [9].

In continuation of our previous studies on thiourea [10], [11], N-[(2,6-Diethylphenyl) carbamothioyl]-2,2-diphenylacetamide (Compound I), N-[(3-Ethylphenyl) carbamothioyl]-2,2-diphenylacetamide (Compound II) and 2,2-Diphenyl-N-{[2-(trifluoromethyl) phenyl]carbamothioyl} acetamide (Compound III) have successfully been synthesized and characterized using FTIR, ^{1}H and ^{13}C NMR and Single Crystal X-Ray analysis. The method used in structural optimize calculation for all compounds is DFT at the basis set levels of B3LYP/6-31G+(2d,p) and B3LYP/6-311G+(2d,p) provide the results of geometrical parameters, fundamental frequencies, GIAO ^{1}H and ^{13}C NMR chemical shift values, and HOMO-LUMO energies. The three dimensional structures and crystal packing of all compounds have been published [12]-[14] but in this report we would like to present the theoretical results of compounds I, II and III in comparison with the experimental data.

II. EXPERIMENTAL

A. Synthesis

For compound I, an acetone (30ml) solution of 2,6-diethylaniline (2.01g, 13.5mmol) was added to a round-bottom flask containing 2,2-diphenylacetyl chloride (3.10g, 13.5mmol) and ammonium thiocyanate (1.03g, 13.5mmol). The mixture was put at reflux for 2.5h then filtered off and left to evaporate at room temperature. The colourless precipitate obtained was washed with water and cold ethanol. Colourless plates were obtained by recrystallization of the precipitate from MeOH solution. Compounds II and III were synthesized with a similar procedure as described in compound I. The

I. A. Razak is with the School of Physics, Universiti Sains Malaysia, 11800 USM, Penang, Malaysia (e-mail: arazaki@usm.my).

S. Arshad and A. A. Rahman are with the School of Physics, Universiti Sains Malaysia, 11800 USM, Penang, Malaysia (phone: 604-653-3438; fax: 604-657-9150; e-mail: sueshad_buntong@yahoo.com, arazhar@usm.my).

N. R. Razali was with the Department of Chemical Sciences, Faculty of Science and Technology, Universiti Malaysia Terengganu, Mengabang Telipot, 21030 Kuala Terengganu, Malaysia (e-mail: mohdsukeri@umt.my).

M. S. M. Yusof is with the Department of Chemical Sciences, Faculty of Science and Technology, Universiti Malaysia Terengganu, Mengabang Telipot, 21030 Kuala Terengganu, Malaysia (e-mail: mohdsukeri@umt.my).

solutions of 3-ethylaniline (1.63g, 13.5mmol) and 2-(trifluoromethyl)aniline (1.25g, 8.4mmol) were used in compound II and III, respectively, as a replacement of 2,6-diethylaniline used in compound I. Colorless crystals suitable for X-ray analysis were obtained by recrystallization.

B. Instrumentation Details

The crystal structures were determined by a single crystal X-ray diffraction from data collected at low temperature (100K) using the Oxford Cryosystem Cobra low-temperature attachment [15]. The data were collected using a Bruker APEX2 CCD diffractometer with the graphite monochromated MoKα (λ= 0.71073 Å) radiation and with APEX2 software [16]. The collected data were reduced using SAINT programme [16]. The empirical absorption corrections were performed by the SADABS programme [16]. The structure was solved by direct methods and refined by full matrix least-squares using the SHELXTL software package [17]. The structure analysis and presentation of the results were made using PLATON [18]. Infrared spectra of the compounds were recorded from KBr discs in the spectral range of 400-4000cm⁻¹ by using FTIR Pelkin-Elmer System 100 Spectrometer. The ^{1}H NMR (400.11 MHz) and ^{13}C NMR (100.61 MHz) spectra were recorded on Bruker Avance III 400 Spectrometer in solution of deuterated dimethyl sulfoxide (DMSO) as solvents at room temperature in the range of 0-15ppm and 0-200ppm. The chemical shifts were also referenced to the trimethylsilyl (TMS) as internal standard.

C. Theoretical Calculation

The molecular geometries were optimized by using Density Functional Theory hybrid method with Becke's nonlocal three parameter exchange and the Lee, Young and Parr correction (B3LYP) using the 6-31G+(2d,p) and 6-311G+(2d,p) basis sets as implemented in the GAUSSIAN 09 program package [19]. The optimized structural parameters were used to calculate the vibrational wavenumbers and isotropic chemical shifts. The gauge-invariant atomic orbital (GIAO) method was used to calculate the ^{1}H and ^{13}C NMR chemical shifts in ppm relative to TMS as internal standard. The GIAO approach allows the computation of the absolute chemical shielding due to the electronic environment of the individual nuclei and this method is often more accurate than those calculated with other approaches for the same basis set [20]. Gauss View molecular visualization program has been used for the animation of vibrational band assignments, HOMO and LUMO diagrams and preparation of the spectrum [21].

III. STRUCTURAL STUDIES

The molecular structures of N-[(2,6-Diethylphenyl) carbamothioyl] -2,2-diphenylacetamide (Compound I), N-[(3-Ethylphenyl) carbamothioyl] -2,2-diphenylacetamide (Compound II) and 2,2-Diphenyl-N-{[2-(trifluoromethyl)phenyl]carbamothioyl}acetamide (Compound III) are shown in Fig. 1. The X-ray crystallography analysis and crystal packing for all compounds have been published [12]-[14]. In order to study their properties at the minimum

energy, the molecular geometries obtained from the X-ray single crystal analysis were optimized to standard convergence criteria in two different basis sets of B3LYP/6-31G+(2d,p) and B3LYP/6-311G+(2d,p). All selected bond lengths and angles are concluded in Table I and the optimized structures of the compounds are shown in Fig. 1. The value of bond lengths and bond angles were in a good agreement with the experimental data except for the hydrogen-attached atoms, which showed higher values than the experimental results. The disagreement between the experimental and theoretical values was due to the environmental factor where the theoretical calculations were performed in gaseous state, whereas the experimental data belonged to the solid phase.

The simulation data for all compounds revealed that the bond lengths of C-N (Table I) are shorter than the normal C-N single bond character (1.48 Å), which also indicates a partial double bond character. The reason for these C-N bonds is because of the resonance effect in this part of the molecules. The same resonance effect was also observed from the C-S bonds [normal C-S single bond = 1.82 Å and normal C=S double bond = 1.56 Å]. All other bond lengths were within the expected range. The partial double bond character of C-N and C-S bonds is shown in the optimized structure [Figs. 1(a)-(f)] by the dashed line. Atiş [21] stated that the bond characters of the structure are presumed as a result of the intramolecular H-bond locking the molecules into a planar six-numbered ring structure. The molecular structures obtained from X-ray Single Crystal Analysis (Fig. 1) have confirmed the existence of intramolecular N—H…O hydrogen bond in all compounds. In addition, for compound II an extra intramolecular C—H…S is observed. The dashed lines (Fig. 1) represent the intramolecular hydrogen bonds and the same bond length character is also observed from the previously reported structure of the same molecular species [10], [11].

The calculated bond angles of all compounds were in a good agreement with the experimental data where the angle differences were between 0 to 2°. The bond angles of C—N—C within the thiourea moiety gave the value range of 120 to 133 where the same range of angles were also reported from the previous studies [21]-[23]. These results show sp^2 hybridization on the N1 and N2 atoms across the C—N—C—N group [24]. In addition, the calculated S—C—N—C—N—O group were essentially planar for all compounds and comparable with the experimental results.

TABLE I
SELECTED BOND LENGTHS AND ANGLES

Compound I				Compound II				Compound III			
Atoms[a]	Experimental	B3LYP /6-31G +(2d,p)	B3LYP/6 -311G +(2d,p)	Atoms	Experimental	B3LYP /6-31G +(2d,p)	B3LYP /6-311G +(2d,p)	Atoms[a]	Experimental	B3LYP /6-31G +(2d,p)	B3LYP /6-311G +(2d,p)
Bond lengths (Å)											
S1–C15	1.675(2)	1.670	1.668	S1–C15	1.662 (3)	1.671	1.669	S1–C15	1.661 (2)	1.667	1.666
O1–C14	1.225(2)	1.224	1.222	O1–C14	1.224 (3)	1.226	1.224	O1–C14	1.216 (2)	1.222	1.220
N1—C14	1.377 (2)	1.377	1.376	N1—C14	1.377 (3)	1.374	1.374	N1—C15	1.337 (3)	1.349	1.347
N1—C15	1.391 (2)	1.409	1.408	N1—C15	1.404 (4)	1.415	1.414	N1—C16	1.435 (2)	1.418	1.418
N1—H1N1	0.850 (2)	1.011	1.010	N1—H1N1	0.820 (3)	1.011	1.010	N1—H1N1	0.960 (3)	1.024	1.023
N2—C15	1.332 (2)	1.340	1.337	N2—C15	1.334 (3)	1.344	1.342	N2—C14	1.369 (3)	1.380	1.379
N2—C16	1.439 (2)	1.437	1.438	N2—C16	1.416 (4)	1.412	1.412	N2—C15	1.405 (2)	1.404	1.403
N2—H1N2	0.860 (2)	1.022	1.021	N2—H1N2	0.900 (3)	1.024	1.023	N2—H1N2	0.807 (2)	1.011	1.010
Bond angles (°)											
C14—N1—C15	128.46 (15)	129.69	129.69	C14—N1—C15	129.1 (2)	130.32	130.35	C15—N1—C16	124.13 (18)	126.26	126.25
C15—N2—C16	124.03 (15)	125.42	125.47	C15—N2—C16	132.1 (3)	132.49	132.43	C14—N2—C15	128.37 (19)	129.82	129.80
C14—C7—C8	109.72 (14)	110.83	111.11	C14—C7—C8	110.1 (2)	110.96	110.75	C14—C7—C8	115.23 (13)	110.66	110.75
C14—C7—C6	109.54 (14)	110.87	110.73	C14—C7—C6	111.0 (2)	110.84	111.02	C14—C7—C6	111.04 (16)	110.89	110.81
O1—C14—N1	122.87 (16)	123.09	123.16	O1—C14—N1	122.6 (3)	122.56	123.16	O1—C14—N2	122.15 (15)	122.85	122.95
O1—C14—C7	123.13 (15)	122.66	122.62	O1—C14—C7	122.7 (2)	123.05	122.52	O1—C14—C7	122.26 (17)	122.87	122.85
N1—C14—C7	113.98 (14)	114.25	114.21	N1—C14—C7	114.7 (2)	114.38	114.32	N2—C14—C7	115.46 (18)	114.27	114.19
N2—C15—N1	116.69 (15)	115.10	115.05	N2—C15—N1	113.7 (2)	113.60	113.57	N1—C15—N2	114.95 (19)	114.48	114.43
N2—C15—S1	124.24 (14)	127.03	127.11	N2—C15—S1	128.4 (2)	130.07	130.11	N1—C15—S1	125.53 (14)	127.75	127.78
N1—C15—S1	119.07 (13)	117.87	117.83	N1—C15—S1	117.9 (2)	116.34	116.32	N2—C15—S1	119.53 (16)	117.76	117.79
Torsion angles (°)											
C15—N1—C14—O1	−2.0 (3)	-0.5	-0.3	C15—N1—C14—O1	−5.2 (5)	-0.6	-0.3	C15—N2—C14—O1	8.3 (3)	-1.0	-1.2
C8—C7—C14—O1	74.7 (2)	81.4	79.7	C8—C7—C14—O1	−13.1 (4)	-46.8	-47.8	C8—C7—C14—O1	128.74 (18)	82.2	82.6
C6—C7—C14—O1	−54.8 (2)	-46.4	-48.3	C6—C7—C14—O1	114.1 (3)	80.8	80.1	C6—C7—C14—O1	2.8 (2)	-45.4	-45.2
C8—C7—C14—N1	−104.4 (2)	-97.8	-99.6	C8—C7—C14—N1	167.0 (2)	134.1	133.1	C6—C7—C14—N2	178.66 (14)	135.6	135.8
C6—C7—C14—N1	126.2(2)	134.4	132.4	C6—C7—C14—N1	−65.8 (3)	-98.2	-99.0	C8—C7—C14—N2	−65.8 (3)	-96.8	-96.4
C16—N2—C15—N1	176.9 (2)	-179.7	-179.9	C16—N2—C15—N1	−176.0 (3)	179.3	179.1	C16—N1—C15—N2	177.55 (15)	178.3	178.8
C16—N2—C15—S1	−3.3 (3)	1.0	0.8	C16—N2—C15—S1	3.2 (5)	-0.4	-0.6	C16—N1—C15—S1	−2.0 (3)	-2.4	-1.9
C14—N1—C15—N2	3.8 (3)	2.3	1.9	C14—N1—C15—N2	2.0 (4)	1.0	0.5	C14—N2—C15—N1	−1.1 (3)	0.3	0.5
C14—N1—C15—S1	−176.0(2)	-178.3	-178.7	C14—N1—C15—S1	−177.3 (2)	-179.3	-179.8	C14—N2—C15—S1	178.46 (14)	-179.1	-178.9
C15—N2—C16—C17	104.9 (2)	100.1	100.2	C15—N2—C16—C17	166.4 (3)	-177.8	-175.7	C15—N1—C16—C17	−65.9 (2)	-52.9	-53.6

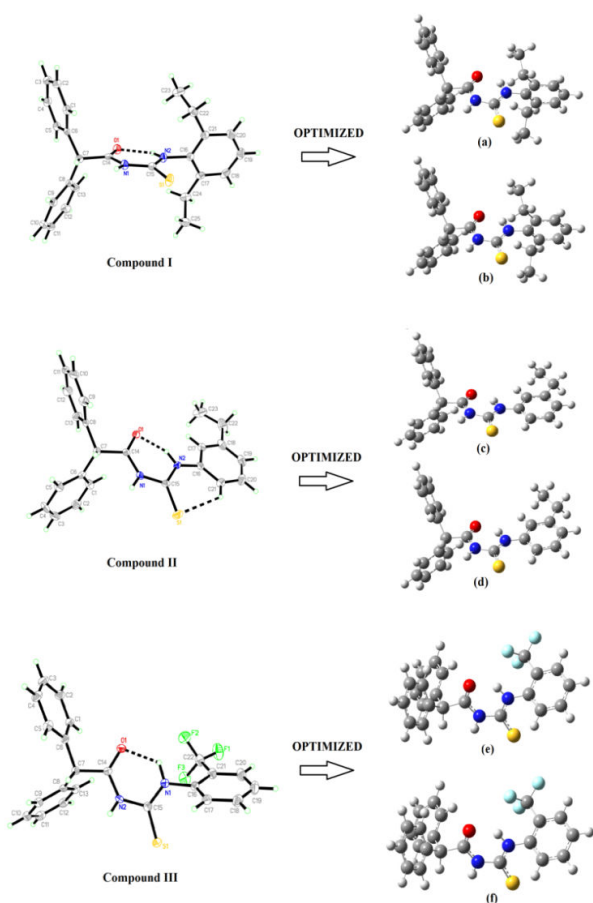[a] The atoms numbering are referred to the X-ray molecular diagram in Fig. 1.

Fig. 1 The molecular structure of Compounds I, II and III obtained from Single Crystal X-Ray Analysis; [(a),(c),(e)] The optimized structure at basis set of B3LYP/6-31G +(2d,p) and [(b),(d),(f)] The optimized structure at basis set of B3LYP/6-311G +(2d,p).

IV. VIBRATIONAL ANALYSIS

The harmonic vibrational frequencies for compounds I, II and III are calculated at B3LYP/6-31+(2d,p) and B3LYP/6-311G+(2d,p) basis. However, the calculated and the experimental frequencies revealed the overestimation of the calculated wavenumbers corresponding to the observed results neglecting the anharmonicity in the real system. In order to improve the agreement with the experiment data, scaling factor of 0.9613 is used to scale down the calculated harmonic wavenumbers. Table II shows the selected experimental frequencies, relative intensities and probable assignments. The presented results discuss only selected important band in carbonyl thiourea group which are:

A. νN-H band

The stretching N–H group was clearly observed in the range of 3220cm^{-1} to 3475 cm^{-1} for B3LYP/6-31G+(2d,p) and of 3216.58 cm^{-1} to 3467.77 cm^{-1} for B3LYP/6-311G+(2d,p), while the experimental vibrational frequencies ranged from 3244.77 cm^{-1} to 3451.44 cm^{-1}. The peaks were clearly found at the most highest values of wavenumbers where these stretching assignments were due to the formation of intra- and intermolecular hydrogen bonds formed by the N–H.

B. νC-O band

The FTIR experimental data show the carbonyl stretching bands were found at the range of 1618.68 to 1684.01 cm^{-1} and the strong calculated carbonyl bands were clearly observed at 1654.40-1672.35 cm^{-1} for both basis sets. These values were decreasing compared to the vibration of carbonyl group (1710 cm^{-1}). The effect of conjugated resonance and the formation of intramolecular N—H…O hydrogen bond within the molecules may have caused the strong C=O stretching bands.

C. νC-N band

The C–N vibrational bands were observed at 1551, 1265 and 1171 cm^{-1} respectively to δ_{CN-H}, $\nu_{C(O)-N}$ and $\nu_{C(S)-N}$ as reported in the related structure of thiourea [22]. In compounds I, II and III, the same values of wavenumbers were found from the experimental data (Table II). The vibration of CN-H bands revealed the existence of intramolecular N—H…O hydrogen bond. Determinations of the C–N vibrational bands were difficult but by the help of DFT method calculations, the stretching C–N vibrations were found and assigned within the same range with the experimental values (Table II).

D. νC-S band

The IR absorptions of C=S band were observed at the range of 692.58 to 699.19 cm^{-1}. The calculated C=S bands were in a good agreement with the experimental results. The calculated C=S bands showed higher values of frequencies observed in compound II. These higher frequency values in compound II may have been due to the formation of an extra intramolecular C—H…S hydrogen bond observed in the molecular structure generated by the X-Ray single crystal analysis.

Fig. 2 presents the linearity between the experimental and calculated vibrational frequency. The computed frequency values usually contain known systematic error and therefore by plotting the correlation graph, the best basis set can be determined. As can be seen from the correlation graphs, obtained correlations were 0.998 for compound I and 0.999 for compounds II and III, and both basis sets gave the same correlation values. In compounds I, II and III, the use of higher basis set did not affect the results of the vibrational studies where the experimental and theoretical results for both basis sets fitted each other well.

TABLE II
SELECTED EXPERIMENTAL AND CALCULATED VIBRATIONAL FREQUENCIES

Experimental (cm^{-1})	Calculated IR (km mol^{-1})						Assignments[a]
	B3LYP 6-31G+(2d,p)			B3LYP 6-311G+(2d,p)			
	Unscaled	Scaled	IR$_{int}$	Unscaled	Scaled	IR$_{int}$	
Compound I							
3445.86	3615.33	3475.42	37.02	3607.38	3467.77	36.60	υNH
3339.02	3406.40	3274.57	359.99	3397.39	3265.91	359.43	υNH
1618.68	1730.48	1663.51	128.61	1719.92	1653.34	125.76	υCO
1520.21	1569.73	1508.98	342.75	1566.37	1505.75	367.65	υCN,ρNH
1374.86	1389.52	1335.75	236.47	1388.51	1334.76	146.91	υCN,ρNH
1149.01	1169.42	1124.16	266.02	1163.90	1118.85	288.55	υCN,ρNH
692.58	698.14	671.12	16.34	697.44	670.45	18.14	υCS
Compound II							
3453.44	3612.87	3473.05	38.52	3604.35	3464.86	38.04	υNH
3293.33	3349.70	3220.07	364.85	3346.07	3216.58	357.58	υNH
1684.01	1730.20	1663.24	101.53	1721.00	1654.40	98.20	υCO
1524.93	1548.54	1488.61	486.04	1542.69	1482.99	456.02	υCN,ρNH
1351.34	1396.68	1342.63	517.78	1389.85	1336.06	357.57	υCN,ρNH
1125.92	1172.56	1127.18	218.07	1167.36	1122.18	243.67	υCN,ρNH
699.19	743.80	715.02	49.09	743.75	714.97	42.73	υCS
Compound III							
3435.54	3615.37	3475.46	38.36	3606.12	3466.56	38.17	υNH
3244.77	3364.05	3233.86	436.08	3356.79	3226.88	433.79	υNH
1676.41	1739.67	1672.35	119.61	1730.58	1663.60	118.28	υCO
1524.78	1539.53	1479.95	495.77	1536.07	1476.62	292.69	υCN,ρNH
1351.61	1348.97	1296.76	153.95	1336.88	1285.14	177.22	υCN,ρNH
1145.81	1176.85	1131.30	256.27	1174.49	1129.03	245.86	υCN,ρNH
697.98	735.09	706.64	41.92	735.13	706.68	38.23	υCS

[a] vibrational assignment of ν, stretching; ρ, rocking.
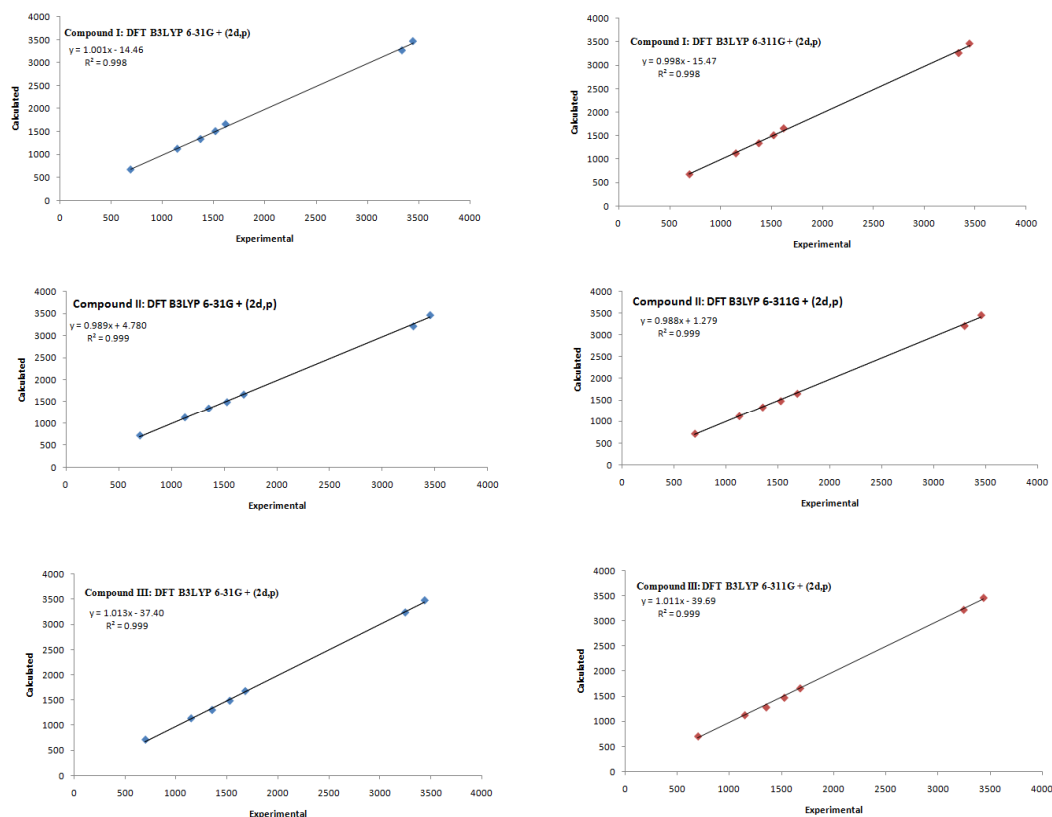

Fig. 2 The linear corrected between the calculation and FT-IR spectrum of compounds I, II and III

V. NMR Analysis

The compounds were calculated by using DFT method with basis sets of B3LYP/6-31G+(2d,p) and B3LYP/6-311G+(2d,p). All the experimental and calculated results are tabulated in Table III. As can be seen from the table, the experimental and theoretical values were in a good agreement where the values had the same range of chemical shift. The results of the calculated values were corrected via the TMS isotropic chemical shift values.

In ^{1}H NMR, the NH resonance can be clearly seen where two single peaks were observed at the most downfield area (11.697 and 11.871ppm in compound I, 11.852 and 12.364 ppm in compound II, and 12.308 and 12.144ppm in compound III). Meanwhile, the calculated chemical shifts showed higher values for about 0.5 to 3.5ppm differences with the experimental results. The high shifted values were due to the presence of strong intramolecular N—H…O hydrogen bonds in the molecules. The calculated chemical shifts for hydrogen attached to isobutene moiety were in the range of 4.2 to 4.5 ppm where the differences were 1ppm with the experimental data. The hydrogen atoms of the aromatic ring, methylene group and methyl group were generally in the normal range and comparable with the experimental data (Table III).

In ^{13}CNMR, δ values of thione group and carbonyl group were 180.73 ($\delta_{C=S}$) and 173.42 ($\delta_{C=O}$) ppm (compound I), 178.57 ($\delta_{C=S}$) and 173.49 ($\delta_{C=O}$) ppm (compound II), and 181.32 ($\delta_{C=S}$) and 173.88 ($\delta_{C=O}$) ppm (compound III). These groups were at the most deshielded area compared to other carbon atoms because of the environmental factor and the increase of electronegativity from sulphur and oxygen atoms. Theoretical values gave variety values of C=S and C=O chemical shift from both basis sets where the difference was almost 1 to 5ppm. Other carbon atoms were located in the same range as the previously reported structures [22], [23] and calculated δ values were in a good agreement with the experimental results.

The results of the ^{1}H and ^{13}C NMR calculated from two different basis sets were not systematic in relation with the experimental results. Even though in the same basis set, there were some values in a very good agreement and there were some that are not. Overall, the calculated chemical shifts were in the normal range and in a good agreement with the experimental results especially of the ^{13}C NMR.

VI. Molecular Orbital Analysis

The highest occupied molecular orbital (HOMO) energy, the lowest unoccupied molecular orbital (LUMO) and the energy gap of HOMO and LUMO for all compounds calculated at two different basis sets, B3LYP/6-31G+(2d,p) and B3LYP/6-311G+(2d,p) are shown in Fig. 3. Analysis on the frontier orbitals of a molecule helped to determine the electrical and optical properties and the steps to react with other molecule [20], [25]. The charge transfer interaction from the ground state (HOMO) to the excited state (LUMO) gave the value of energy gap (ΔE) where the smaller the band gap, the higher the stability of the molecule.

As observed in Fig. 3, the charge density of HOMO for all compounds mainly accumulated on the C=S group and small parts from its neighbouring atoms. In the excited state (LUMO), the charge density mostly delocalized within the carbonyl-thiourea moiety. Higher surface charges were located at sulphur and nitrogen atoms, which had the potential to act as coordination points. For basis set B3LYP/6-31G+(2d,p), the energy gap of compounds I, II and III were 4.455866117, 4.297495791 and 4.313550514 eV respectively. Meanwhile, basis set B3LYP/6-311G+(2d,p) gave the values of energy gap of 4.453689205 (Compound I), 4.311373603 (Compound II) and 4.315727426 (Compound III) eV. The same range of energy gap values were observed from both basis sets but there were differences in the dipole moment values. Compounds I and II gave the values of the dipole moments ranging from 2.9714 to 3.2557 Debye, whereas, in compound III the dipole moment values were 1.9989 and 1.9616 Debye for both basis sets. These differences were perhaps due to the different substituent groups attached to the phenyl ring that affected the molecular polarization where the triflouromethyl group in compound III is often described to have more significant electronegativity character as to be compared to the propane group.

VII. Conclusion

The crystal structure of compounds I, II and III were synthesized and characterized by X-Ray Crystallography analysis, FT-IR and NMR spectroscopy. The optimized molecular structure for all compound were calculated using DFT/B3LYP6-31G+(2d,p) and DFT/B3LYP6-311G+(2d,p) basis sets along with the vibrational frequencies and the isotropic chemical shift. The calculated parameters from the DFT/B3LYP6-311G+(2d,p) and DFT/B3LYP6-31G+(2d,p) basis set gave good agreement in all the experimental data. The correlation values of 0.998 and 0.999 were obtained from the vibrational frequency studies. The chemical shift obtained from the ^{13}C NMR was in a very good agreement with the experimental data. Compound II gave the smallest energy gap (4.29eV and 4.31eV) as compared to compounds I and III. The energy gap values for all compounds ranged at the same values where the compounds may have had the potential for optical and electronic properties. The different substituent groups attached to benzene ring did not affect the energy of the compounds but they did affect the values of the dipole moment, where compound III had the smallest values of dipole moments from both basis sets.

TABLE III
THE EXPERIMENTAL AND CALCULATED NMR CHEMICAL SHIFT

^{1}H NMR				^{13}C NMR			
Atoms [a]	Experimental	B3LYP 6-31G + (2d,p) [b]	B3LYP 6-311G + (2d,p) [c]	Atoms [a]	Experimental	B3LYP 6-31G + (2d,p) [b]	B3LYP 6-311G + (2d,p) [c]
Compound I							
N1-H1N1	11.697	8.609	8.5017	C14	173.42	168.295	176.545
N2-H1N2	11.871	11.6731	11.4356	C15	180.73	179.492	189.412
Aromatic Proton	7.410-7.301, 7.241, 7.138	8.2499, 7.773, 7.6989, 7.6188, 7.5665, 7.5498, 7.5467, 7.4273, 7.4087, 7.3971, 7.3305, 7.3056, 7.2295	8.3527, 7.8229, 7.7096, 7.6279, 7.6049, 7.4926, 7.4723, 7.4378, 7.4278, 7.4113, 7.3659, 7.3624, 7.2626	C6,C8	138.57	137.015, 133.667	146.233, 143.517
Proton of Isobutane	5.513	4.3521	4.4972	C1,C5,C9, C13	128.56	126.814, 124.998, 124.756, 121.747	134.889, 133.675, 132.135, 131.401
Methylene	2.501	2.9539, 2.8729, 2.3516, 2.3353	2.994, 2.8099, 2.3688, 2.3249	C2,C4,C12, C10	128.60	128.173, 127.992, 125.197, 123.837	132.961, 132.832, 132.688, 132.267
Methyl	1.119	1.4567, 1.0899, 1.0247, 0.8800, 0.8408, 0.8231	1.3985, 1.0692, 0.9846, 0.8486, 0.8248, 0.7909	C3,C11	127.95	124.536, 123.641	131.905, 131.508
				C7	56.39	64.634	67.1749
				C16	134.77	132.47	140.644
				C17,C21	140.61	141.485, 140.290	151.064, 149.432
				C18,C20	126.20	125.1, 125.058	132.202, 132.022
				C19	127.28	126.043	132.803
				C22,C24	24.22	30.955, 30.863	31.077, 30.893
				C25,C23	14.25	19.254, 18.895	18.243, 17.538
Compound II							
N1-H1N1	11.852	8.2566	8.0816	C14	173.49	169.028	175.724
N2-H1N2	12.364	13.1386	12.8749	C15	178.57	172.425	182.051
Aromatic Proton	7.520, 7.458-7.280, 7.101	9.5659, 8.3608, 8.0119, 7.6157, 7.5782, 7.5086, 7.5026, 7.4823, 7.4648, 7.4531, 7.4226, 7.3484, 7.1529, 6.9157	9.6218, 8.2839, 7.7411, 7.6551, 7.5324, 7.5168, 7.5066, 7.4592, 7.4490, 7.4445, 7.3756, 7.3215, 7.1353, 6.9291	C6,C8	137.62	136.281, 135.943	145.704, 144.568
Isobutane proton	5.499	4.2235	4.4160	C1,C5,C9, C13	128.64	126.61, 126.481, 124.466, 122.836	134.891, 133.776, 132.302, 130.372
Methylene	2.605	2.9099, 2.8378	2.8906, 2.8665	C2,C4,C12, C10	128.58	126.012, 125.93, 125.742, 124.777	133.451, 133.101, 132.48, 131.611
Methyl	1.175	1.2869, 1.2703, 1.2311	1.2510, 1.2168, 1.2047	C3,C11	127.29	124.691, 124.086	131.868, 131.654
				C7	56.32	65.570	67.054
				C16	138.41	136.469	144.819
				C17	123.45	113.867	119.833
				C18	144.38	139.507	149.203
				C19	125.81	123.465	130.197
				C20	128.45	125.436	132.434
				C21	121.44	113.460	119.590
				C22	27.92	29.505	29.767
				C23	15.33	12.255	10.999
Compound III							
N1-H1N1	12.308	12.5667	12.2618	C14	173.88	168.796	175.889
N2-H1N2	12.144	8.6887	8.4601	C15	181.32	177.804	188.092
Aromatic Proton	7.776, 7.720, 7.526, 7.410-7.303	8.3538, 8.1685, 7.921, 7.6812, 7.6563, 7.6319, 7.5684, 7.564, 7.4895, 7.4695, 7.4442, 7.4269, 7.4053, 7.3634	8.2345, 8.0911, 7.8824, 7.7406, 7.666, 7.585, 7.5031, 7.4974, 7.496, 7.4352, 7.4312, 7.429, 7.4065, 7.3117	C6,C8	138.32	137.353, 135.209	145.427, 143.107
Isobutane proton	5.529	4.4698	4.4676	C1,C5,C9, C13	128.62	128.332, 125.491, 124.064, 122.587	134.019, 134.00, 132.245, 130.796
				C2,C4,C12, C10	127.80	127.069, 126.722, 126.09, 124.741	133.41, 132.989, 132.458, 132.354
				C3,C11	124.82	124.618, 124.186	132.134, 131.515
				C7	56.37	64.0549	66.7346
				C16	135.60	134.358	142.854
				C17	127.34	127.709	134.789
				C18	128.13	128.167	135.175
				C19	124.12	123.090	129.516

C20	124.45	123.664	129.756
C21	124.36	123.099	131.167
C22	130.82	130.666	135.311

[a] The atoms numbering are referred to the X-ray molecular diagram in Fig. 1

[b] The isotropic chemical shift with respect to Tetramethysilane (TMS) in B3LYP 6-31G + (2d,p) are 31.6143 ppm for ^{1}H NMR and 191.2113 ppm for ^{13}C NMR.

[b] The isotropic chemical shift with respect to Tetramethysilane (TMS) in B3LYP 6-311G + (2d,p) are 31.8821 ppm for ^{1}H NMR and 182.4656 ppm for ^{13}C NMR.
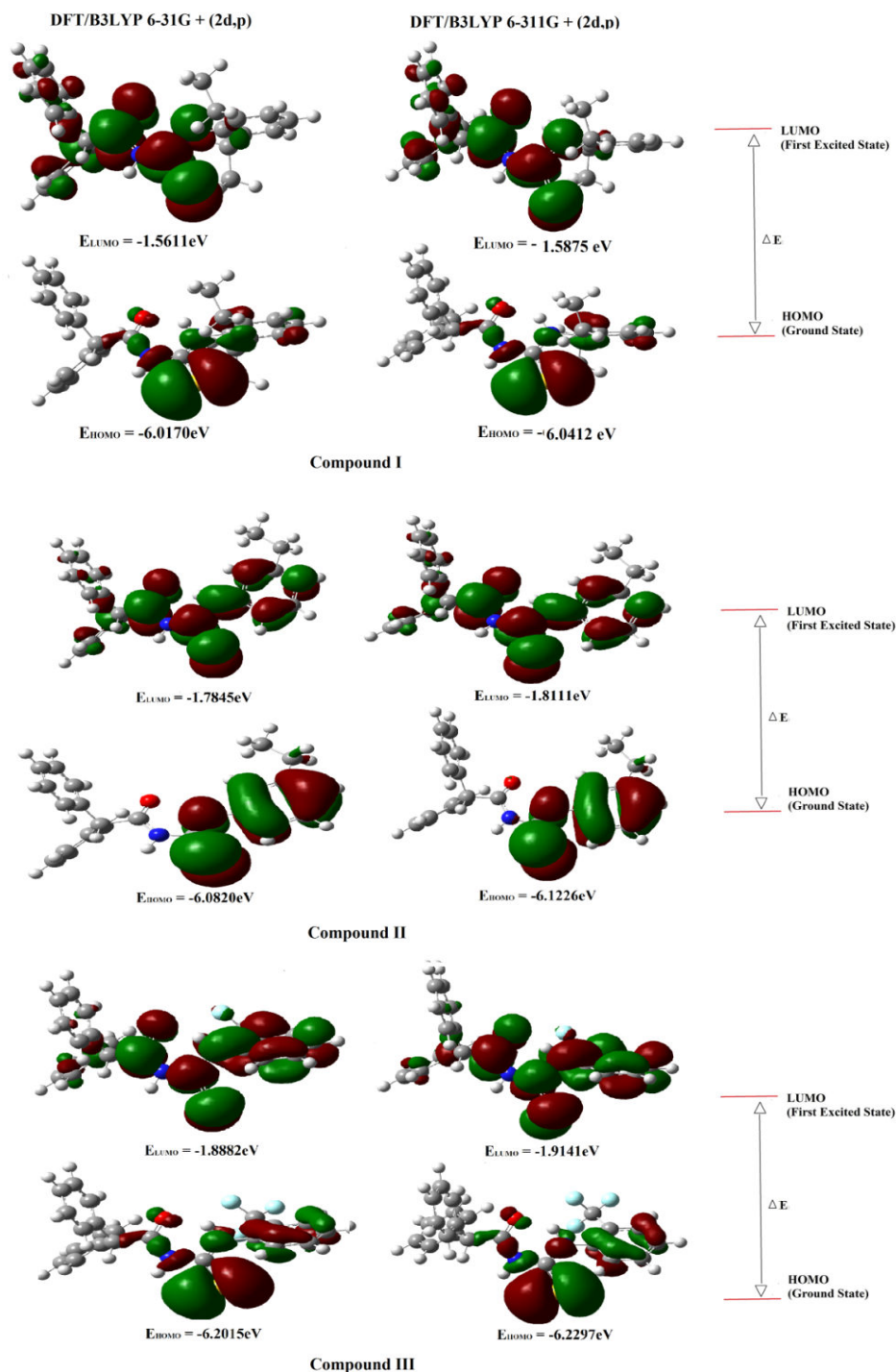

Fig. 3 The atomic orbital composition of the frontier molecular orbital of Compounds I, II and III

REFERENCES

[1] M. G. Babashkina, D. A. Safin, K. Robeyns and Y. Garcia, "Influence of polymorphism on *N*-thiophosphorylated thiourea 4-Me$_2$NC$_6$H$_4$NHC(S)NHP(S)(OiPr)$_2$ crystal design," Inorganic Chemistry Communications, vol 18, pp. 34-37, 2012.

[2] A. Saeed, M. F. Erben and U. Flörke, "Effect of fluorine substitution on the crystal structures and vibrational properties of phenylthiourea isomers," Journal of Molecular Structure, vol 982, pp. 91-99, 2010.

[3] N. Selvakumaran, S. W. Ng, E. R.T. Tiekink and R. Karvembu, "Versatile coordination behavior of *N,N*-di(alkyl/aryl)-*N'*-benzoylthiourea ligands: Synthesis, crystal structure and cytotoxicity of palladium(II) complexes," Inorganica Chimica Acta, vol 376, pp. 278-284, 2011.

[4] M. K. Rauf, Imtiaz-ud-Din,A. Badshah, M. Gielen, M. Ebihara, D. de Vos and S. Ahmed, "Synthesis, structural characterization and *in vitro* cytotoxicity and anti-bacterial activity of some copper(I) complexes with N,N′-disubstituted thioureas," Journal of Inorganic Biochemistry, vol 103, pp. 1135-1144, 2009.

[5] R. del Campo, J. J. Criado, R. Gheorghe, F. J. González, M. R. Hermosa, F. Sanz, J. L. Manzano, E. Monte and E. Rodríguez-Fernández, "*N*-benzoyl-*N*′-alkylthioureas and their complexes with Ni(II), Co(III) and Pt(II) – crystal structure of 3-benzoyl-1-butyl-1-methyl-thiourea: activity against fungi and yeast," Journal of Inorganic Biochemistry, vol 98, pp. 1307-1314, 2004.

[6] S. Saeed, N. Rashid, M. Ali, R. Hussain and P. G. Jones, "Synthesis, spectroscopic characterization, crystal structure and pharmacological properties of some novel thiophene-thiourea core derivatives," European Journal of Chemistry, vol 1, pp. 221-227, 2010

[7] S. Saeed, N. Rashid, P. G. Jones, M. Ali and R. Hussain, "Synthesis, characterization and biological evaluation of some thiourea derivatives bearing benzothiazole moiety as potential antimicrobial and anticancer agents," European Journal of Medicinal Chemistry, vol 45, pp. 1232-1331, 2010.

[8] P. C. Nair and M. E. Sobhia, "Quantitative structure activity relationship studies on thiourea analogues as influenza virus neuraminidase inhibitors," European Journal of Medicinal Chemistry, vol 43, pp. 293-299, 2008.

[9] H. Arslan, U. Flörke, N. Külcü and G. Binzet, "The molecular structure and vibrational spectra of 2-chloro-*N*-(diethylcarbamothioyl)benzamide by Harthree-Fork and density functional methods," Spectrochemica Acta Part A, vol 68, pp. 1347-1355, 2007.

[10] M. S. M. Yusof, S. Arshad, I. A. Razak and A. A. Rahman, "4-*tert*-Butyl-N-[(2,6-dimethylphenyl)-carbamothioyl]benzamide" Acta Crystallographica Section E, vol 68, pp o2670, 2012.

[11] M. S. M. Yusof, N. F. Embong, S. Arshad and I. A. Razak, "*N*-(4-Chlorobutanoyl)-*N*′-[2-(trifluoromethyl) phenyl]thiourea" Acta Crystallographica Section E, vol 68, pp. o1029, 2012.

[12] M. S. M. Yusof, N. R. Razali, S. Arshad, A. A. Rahman and I. A. Razak, "*N*-[(2,6-Diethylphenyl)carbamothioyl]-2,2-diphenylacetamide" Acta Crystallographica Section E, vol 69, pp o967, 2013.

[13] M. S. M. Yusof, N. R. Razali, S. Arshad, A. A. Rahman and I. A. Razak, "*N*-[(3-Ethylphenyl)carbamothioyl]-2,2-diphenylacetamide" Acta Crystallographica Section E, vol 69, pp o1016-o1017, 2013.

[14] M. S. M. Yusof, N. R. Razali, S. Arshad, A. A. Rahman and I. A. Razak, "2,2-Diphenyl-*N*-{[(2-(trifluoromethyl)phenyl]carbamothioyl}acetamide" Acta Crystallographica Section E, vol 69, pp o1255-o1256, 2013.

[15] J. Cosier and A. M. Glazer, *J. Appl. Cryst.*, vol 19, pp. 105-107, 1986.

[16] Bruker. *SADABS, APEX2 and SAINT*. Bruker AXS Inc.: Madison, Wisconsin, USA. 2009

[17] *G. M, Sheldrick, Acta Cryst. A*, vol 64, pp. 112-122, 2008.

[18] *A. L. Spek, Acta Cryst.* D, vol 65, pp. 148-155, 2009.

[19] Gaussian 09, Revision A.1, M. J. Frisch, G. W. Trucks, H. B. Schlegel, G. E. Scuseria, M. A. Robb, J. R. Cheeseman, G. Scalmani, V. Barone, B. Mennucci, G. A. Petersson, H. Nakatsuji, M. Caricato, X. Li, H. P. Hratchian, A. F. Izmaylov, J. Bloino, G. Zheng, J. L. Sonnenberg, M. Hada, M. Ehara, K. Toyota, R. Fukuda, J. Hasegawa, M. Ishida, T. Nakajima, Y. Honda, O. Kitao, H. Nakai, T. Vreven, J. A. Montgomery, Jr., J. E. Peralta, F. Ogliaro, M. Bearpark, J. J. Heyd, E. Brothers, K. N. Kudin, V. N. Staroverov, R. Kobayashi, J. Normand, K. Raghavachari, A. Rendell, J. C. Burant, S. S. Iyengar, J. Tomasi, M. Cossi, N. Rega, J. M. Millam, M. Klene, J. E. Knox, J. B. Cross, V. Bakken, C. Adamo, J. Jaramillo, R. Gomperts, R. E. Stratmann, O. Yazyev, A. J. Austin, R. Cammi, C. Pomelli, J. W. Ochterski, R. L. Martin, K. Morokuma, V. G. Zakrzewski, G. A. Voth, P. Salvador, J. J. Dannenberg, S. Dapprich, A. D. Daniels, Ö. Farkas, J. B. Foresman, J. V. Ortiz, J. Cioslowski, and D. J. Fox, Gaussian, Inc., Wallingford CT, 2009.

[20] M. Atiş, F. Karipchi, B. Sariboğa, M. Taş and H. Çelik, "Structural, antimicrobial and computational characterization of 1-benzoyl-3-(5-chloro-2-hydroxyphenyl)thiourea," Spectrochimica. Acta Part A: Molecular and Biomolecular Spectroscopy, vol 98, pp. 290-301, 2012.

[21] GaussView, Version 5, R. Dennington, T. Keith and J. Millam, *Semichem Inc.*, Shawnee Mission KS, 2009.

[22] X.-E. Duan, X.-H. Wei, H.-B. Tong, S.-D. Bai, Y.-B Zhang, D.-S. Liu, "Ferrocene-modified pyrimidinyl acyl-thiourea derivatives: Synthesis, structures and electrochemistry," Journal of Molecular Structure, vol 1005, pp. 91-99, 2011.

[23] O. Hritzová, J. Černák, P. Šafař, Z. Frőhlichová and I. Csőregh, "Furan derivatives of substituted phenylthiourea: spectral studies, semi-empirical quantum-chemical calculations and X-ray structure analyses" Journal of Molecular Structure, vol 743, pp. 29-48, 2005.

[24] H. Arslan, D. S. Mansuroglu, D. VanDerveer and G. Binzet, "The molecular structure and vibrational spectra of *N*-(2-,2-diphenylacetyl)-*N*'-(naphthalene-1yl)-thiourea by Harthree-Fork and density Functional methods," Spectrochemica Acta Part A: Molecular and Biomolecular Spectroscopy, vol 72, pp. 561-571, 2009.

[25] N. B. Arslan, C. Kazak and F. Aydin, "*N*-(4-Nitrobenzoyl)-*N*'-(1,5-dimethyl-3-oxo-2-phenyl-1*H*-3(2*H*)-pyrazolyl)-thiourea hydrate: Synthesis, spectroscopic characterization, X-ray structure and DFT studies," Spectrochemica Acta Part A: Molecular and Biomolecular.